COMPRESSIVE RESIDUAL STRENGTH OF GRAPHITE/EPOXY LAMINATES AFTER IMPACT

Teresa A. Guy[1] and Paul A. Lagace
Technology Laboratory for Advanced Composites
Department of Aeronautics and Astronautics
Massachusetts Institute of Technology

S11-24

51379

P-22

ABSTRACT

The issue of damage tolerance after impact, in terms of the compressive residual strength, was experimentally examined in graphite/epoxy laminates using Hercules AS4/3501-6 in a $[\pm45/0]_{2S}$ configuration. Three different impactor masses were used at various velocities and the resultant damage measured via a number of nondestructive and destructive techniques. Specimens were then tested to failure under uniaxial compression. The results clearly show that a minimum compressive residual strength exists which is below the open hole strength for a hole of the same diameter as the impactor. Increases in velocity beyond the point of minimum strength cause a difference in the damage produced and cause a resultant increase in the compressive residual strength which asymptotes to the open hole strength value. Furthermore, the results show that this minimum compressive residual strength value is independent of the impactor mass used and is only dependent upon the damage present in the impacted specimen which is the same for the three impactor mass cases. A full three-dimensional representation of the damage is obtained through the various techniques. Only this three-dimensional representation can properly characterize the damage state that causes the resultant residual strength. Assessment of the state-of-the-art in predictive analysis capabilities shows a need to further develop techniques based on the three-dimensional damage state that exists. In addition, the need for damage "metrics" is clearly indicated.

INTRODUCTION

As the use of advanced composite materials for primary structure in the aerospace and aircraft industries increases, concerns involving their damage tolerance need to be further addressed. This, in part, has led to a considerable amount of work on the subject of impact.

There are two issues involved in the subject of impact: damage resistance and damage tolerance [1]. The former deals with the actual impact event and the damage that results; the latter deals with the ability of the composite laminate to perform its desired function (e.g., carry load or retain stiffness) in the presence of damage. The latter is the main topic of the current work.

The importance of the damage size and its location increases with the complexity of the applied stress field. The most significant effects are due to damage in areas subject to high in-plane compression, shear stress, interlaminar stress, or out-of-plane bending moments [2–6]. Of the aforementioned complex stress fields, in-plane compression was

---

[1] currently at *McDonnell Douglas Technologies Incorporated*

selected as the load condition of interest for this work. Experimental evidence shows that a more severe reduction in compressive residual strength occurs from impact damage than due to the presence of an imbedded delamination with equal area (as determined by ultrasonic evaluation) [7–14]. Impact damage may also result in a more severe reduction in compressive residual strength than a hole with an equivalent diameter [6–9, 15, 16]. It is thus important to test configurations with actual impact damage rather than "simulated" damage to get an accurate evaluation of the potential loss in compressive load-carrying ability.

In the great majority of work on impact damage tolerance, researchers have attempted to correlate the post-impact strength with easily measured parameters [e.g., 9, 11, 17–21]. These parameters include planar damage area and impactor metrics (mass, velocity, energy). These results have generally shown that the compressive residual strength exhibits asymptotic behavior as damage area increases and as impactor energy increases. In at least one case [20], an apparent minimum compressive residual strength exists below an equivalent impactor diameter open hole strength value. Preliminary data [22] indicates such a minimum does exist. Furthermore, recent work by Dost, Ilcewicz, and Gosse [23] indicates the need for a full three-dimensional description of the damage state in order to properly determine the residual strength of the laminate. This indicates a need for basic understanding of the damage mechanisms which are important in controlling compressive residual strength. Thus, the main thrust of the current work is the determination of the minimum post-impact compressive residual strength and the damage state which causes it.

OBJECTIVES AND APPROACH

The specific purpose of the work was to provide answers to the following questions (in the context of the specific laminate investigated): one, what is the three-dimensional damage state that governs minimum compressive residual strength behavior; two, is this minimum compressive residual strength value dependent upon impactor mass; and, three, how does this minimum compressive residual strength value relate to impactor mass and velocity?

All laminates were made from AS4/3501-6 graphite/epoxy unidirectional tape manufactured by Hercules, Inc. in a [±45/0]$_{2S}$ configuration. This laminate orientation and material system were selected because of extensive data available on damage resistance and tensile residual strength [e.g., 24]. Three different impactor masses were chosen: 1523 g, 578 g, and 8.4 g. The masses selected are representative of a range of potential impactor masses such as a dropped hand tool down to runway debris kick-up for an aircraft. The first item of the experimental program was the determination of the impactor velocity which resulted in the minimum compressive residual strength for each mass. Preliminary work [22] indicated that with a mass of 8.4 g, minimum compressive residual strength occurs due to the damage incurred at an impactor velocity of 57 m/s. This work also defined the range of velocities which causes from little or no damage to complete penetration of the specimens. (Complete penetration is defined as the tip of the impactor progressing beyond the back surface of the laminate.) Based on this, a number of impactor velocities, shown in Table 1, was chosen for each mass.

After minimum compressive residual strengths were characterized for the three impactor masses of interest, the focus shifted to defining the damage state at these

minima. The intent was to impact specimens at several velocities surrounding the minimum compressive residual strength velocity previously determined. For each impactor velocity, several specimens were destructively evaluated while others were tested for compressive residual strength for corroboration with initial test results. The need for accurate damage assessment to understand the effect of impact damage on compressive residual strength is well-documented [9, 19, 23]. Proponents of destructive evaluation methods [e. g., 25] argue that nondestructive evaluation (NDE) methods are severely limited in defining delamination at ply interfaces and only destructive methods can accurately determine the internal damage state. However, destructive methods are not an option for evaluation of composite structure in a production article nor are they useful when residual strength tests are to be subsequently conducted. Thus, nondestructive methods are being upgraded to accurately determine the through-the-thickness damage state. To that end, both destructive and nondestructive damage evaluation techniques were used in this study to characterize damage in some of the coupons subject to impact. All impact coupons were inspected by at least two NDE techniques: visual inspection, X-ray or ultrasonic scanning. Visual inspection and X-ray were methods used in all cases. Coupon sectioning and the deply technique were the destructive methods of damage evaluation. The different damage evaluation techniques were applied to compare accuracy and adequacy of information provided by the various methods. The full test matrix indicating the different types of damage evaluation techniques used for each specimen is shown in Table 1.

In addition to the impact-damaged compressive residual strength specimens, undamaged specimens and specimens with open holes were tested to provide baseline data. This test matrix is shown in Table 2. The 12.7 mm diameter hole is identical to the diameter of all impactors used in this work. Larger diameter holes were also tested to compare the compressive residual strength after impact to holes larger than the diameter of the impactor. The 25.4 mm diameter hole is the maximum size used in order to avoid finite width effects.

PROCEDURES

Coupon Preparation

All laminates were cured in an autoclave using the manufacturer's recommended cure cycle with a one-hour hold at 117°C followed by a two-hour hold at 177°C. A full vacuum and a pressure of 0.59 MPa was also maintained during the cure. All laminates also underwent an eight-hour postcure at 177°C. Laminates were subsequently cut to a specimen size of 70 mm wide by 340 mm long using a water-cooled diamond blade and were ready for impact or drilling after appropriate measurements were taken.

Impact

Two different impact test methods were used. For each, the test coupons were identical and a common holding jig, illustrated in Figure 1, was used. The holding jig includes a large aluminum plate with a rectangular opening; aluminum bars (in this case, square bars to simulate clamped boundary conditions); and threaded rods with hex nuts used to apply consistent torque (11.3 Nm) at each nut for each test.

The first impact test apparatus consists of a striker unit and an impactor unit, as shown in Figure 2. This apparatus was used with the higher impactor masses (578 g and 1523 g). A 12.7 mm diameter hemispherical steel tup was used in this work and was connected to a steel rod for the 1523 g mass case, and an aluminum rod for the 578 g mass case. A 13 mm thick plastic doughnut that acted as a timing flag was attached to the impactor rod. Impactor velocity was measured by determining the time the plastic doughnut interrupted an LED mounted between the linear bearings on the impactor unit.

The second impact device, as shown in Figure 3, was an air gun initially developed and used at NASA Langley Research Center [26]. This was used for the low mass (8.4 g) impacts. This test apparatus consists of a variable pressure source, a low pressure reservoir, a solenoid trigger, a gun barrel, and 12.7 mm diameter spherical projectiles (steel balls were used in this work). The impactor velocity is measured with an LED system. The projectile passes an infrared LED that sends a signal to the optical trigger box that triggers the timing mechanism. When the projectile passes a second infrared LED, located 200 mm further along the gun barrel, another signal is sent to the optical trigger box to stop the timing mechanism. The time to transverse the two LED's is recorded in each test.

Damage Detection

All of the impact coupons were evaluated by two nondestructive techniques. After visual inspection, X-ray photography was conducted. An enhancing agent of 1,4-Diiodobutane (DiB) was injected into the damaged area with a syringe until a small bubble appeared on the surface of the graphite/epoxy coupon. As DiB is a low viscosity liquid that penetrates into any exposed crack through capillary action, X-rays were taken after a minimum of one hour elapsed time from injection. A typical X-ray photograph of impact damage is presented in Figure 4. A schematic of the damage regions defined by X-ray evaluation is illustrated in Figure 5. The major and minor axes of damage were measured as well as the dimensions of the central region or "core" damage defined by the very dark internal region, indicative of the region of intense fiber damage.

Pulse-echo ultrasonic scanning was performed by Hercules, Inc. with a Metro Tek C403 ultrasonic scanning system. All scanning was performed at a pulse frequency of 10 MHz. A typical ultrasonic C-Scan provided a map of the damage "smeared" through-the-thickness such that the through-the-thickness location(s) of the damage(s) was not indicated. This "two-dimensional" inspection was performed on all specimens that underwent ultrasonic evaluation. In addition, three-dimensional ultrasonic C-Scan data was provided on a ply-by-ply basis for a number of specimens. In these time-of-flight C-Scans, only reflections at the ply of interest are "gated" and thus cause a signal to be received. These reflections occur at damage in the laminate. If there is no damage at the ply, no signal is received within the "gate". Because all plies were not of uniform thickness and the "time" thickness measurement of the laminate was divided by 12 to evaluate each ply, exact location within a ply is not known. The location is known to be within a ply but is unlikely to coincide exactly with a ply interface. Furthermore, if the signal is reflected before the ply, indicative of damage above that location, the area beneath the reflection will be "shadowed" in that little signal will be transmitted. Thus, even if damage at that ply exists, the reflected signal amplitude will be small and will result in no indication of damage.

After X-ray and ultrasonic scanning evaluation, several of the impact coupons were sectioned, as indicated in Table 1. At least five widthwise cuts were made per coupon with a water-cooled diamond blade, the first of which was through the center of impact. The center of impact was located by visual inspection upon placement of the coupon in the milling machine. Delaminations and fiber breaks were measured by examination of the cross-sections under a microscope at 30X magnification. A typical edge through the center of impact is shown in Figure 6. The measurements from all surfaces exhibiting damage were transcribed to schematics of damage on a ply-by-ply basis.

The deply technique [25], another destructive evaluation method, was used on a number of coupons as indicated in Table 1. The enhancing agent used in this work was a solution composed of 10 g of gold chloride in 100 ml of isopropyl alcohol. Thirty minutes after syringe injection of the enhancing agent into the damage region, the coupons were placed into an oven at 66°C for thirty minutes to drive off the excess carrier. Trimmed coupons, containing only the damaged area, were placed on a stainless steel wire mesh in a Lindbergh Furnace (Type 51442) preheated to 415–420°C. A positive pressure of nitrogen gas at approximately 0.02 MPa was fed into the furnace with a vent to an exhaust hood to remove the possibility of the harmful effects of oxygen. Partial pyrolysis of the coupons occurred after forty-five minutes (thirty minutes for eight plies [25]). The laminates were unstacked using a wide strip of transparent tape placed over the top ply (beginning with the impact surface ply). The ply was gently worked free from the specimen exposing the next interface. This was repeated until all plies were separated. However, plies 6 and 7 are both at 0° orientation and were impossible to separate.

The view of damage in the specimens evaluated by the deply technique is from the back surface towards the impact surface which is opposite of the time-of-flight ultrasonic C-Scans and cross-section schematics. Thus, the ply angles are reflected about the vertical axis. Plies were numbered sequentially beginning with the ply opposite the impact surface. Evaluation of the damage types (i.e., delamination and fiber damage) and sizes was done by visual inspection with a bright light shined on the ply to reflect the gold chloride. Photographs were then taken to provide a record of damage. A typical photograph is shown in Figure 7. There was obvious fiber damage in this ply where the tup passed through the coupon as evidenced by the white background in the photograph. The gold chloride, providing evidence of delamination where ply 1 (back surface from impact) separated from ply 2, typically appeared gray compared to the white of the background and the black of the graphite/epoxy.

After the impact coupons were evaluated by the prescribed destructive and nondestructive methods, details of the identified damage were compared. The C-Scan damage definition was directly comparable to X-ray results. The time-of-flight C-Scan damage definition was comparable to the schematics generated by cross-sectioning and the photographs from the deply evaluation. Extensive documentation and comparison of destructive and nondestructive damage evaluation methods are presented in Reference 27 and will be the topic of a future paper.

Determination of Compressive Residual Strength

After nondestructive damage evaluation, specimens were prepared for compressive residual strength tests. A honeycomb sandwich specimen, shown in Figure 8 and

designed for characterization of the compressive strength of thin laminates [28], was used. Placement of the 25 mm thick honeycomb core between the two facesheets prevented global buckling of the laminate as a possible failure mode. The core was a combination of low density (72 kg/m^3) and high density (352 kg/m^3) aluminum honeycomb. The high density core was located in the grip area to prevent crushing of the specimen when it is held in the hydraulic grips of the test fixture. The core located in the test section was low density to virtually eliminate load-sharing with the facesheets.

The impacted coupon and an undamaged coupon were bonded to this aluminum honeycomb core after impact and nondestructive evaluation. The impacted surface was bonded to the honeycomb as it was smoother than the back surface with splinters and more likely to result in a good bond. American Cyanimid FM-123-2 film adhesive was used for bonding with a cure temperature of 107°C and pressure of 0.28 MPa for two hours. Using the same adhesive and cure cycle, fiberglass end tabs were then bonded to the graphite/epoxy to provide an efficient load transfer mechanism. Coupons with drilled holes, rather than impact damage, were also fabricated into identical compressive residual strength test specimens. Holes were drilled using diamond-coated drill bits and reamers. A strain gage was placed on the damaged facesheet, away from the damage, to provide data that was used as a specimen quality check through laminate stiffness measurement.

Tests were conducted using an MTS 810 Material Testing System under stroke control at a rate of 1.1 mm/min. This resulted in an approximate strain rate of 5000 microstrain/min in the test section. The tests were conducted monotonically to failure. Failure stress is calculated by dividing the failure load of the damaged facesheet by the measured area (average thickness and width). The failure load of the damaged facesheet is half the total column load at failure.

RESULTS AND DISCUSSION

Minimum Compressive Residual Strength

Residual strength data is often presented as a function of impactor velocity or energy. This presentation method complicates interpretation of results for different laminates or material systems as the issues of damage resistance and damage tolerance are not separately addressed. Thus, to address damage resistance, damage size as a function of impactor energy or velocity should also be provided. In this work, presentation of residual strength as a function of impactor velocity was used to determine the minimum compressive residual strength. Impactor velocity was the parameter then used in an attempt to repeat the damage state causing minimum compressive residual strength for intensive destructive damage evaluation.

The results of compressive residual strength versus impactor velocity for the cases of the three impactor masses are summarized in the left graph in Figure 9. All three data sets indicate a minimum compressive residual strength below the compressive strength for specimens with open holes. Furthermore, all three data sets exhibit asymptotic behavior approaching the strength value for the open hole of the same diameter as the impactor. (The results of the open hole and undamaged strength tests were presented in Table 2.) The right graph in Figure 9 is a plot of the same data on a scale of 0–15 m/s to better show the aforementioned trends for the 1523 g and 578 g

impactor mass cases. The minimum compressive residual strengths exhibited in the three data sets are: 184 MPa for the 1523 g mass at 6.3 m/s, 191 MPa for the 578 g mass at 9.2 m/s, and 187 MPa for the 8.4 g mass at 57 m/s. The three impactor masses, at their respective minimum compressive residual strength velocities, therefore caused virtually identical minimum compressive residual strengths. Thus, minimum compressive residual strength is apparently independent of impact mass.

Although it has been shown that impactor energy is not a sufficient metric [1], residual strength results are often presented as a function of impactor energies. However, in this current work, impactor energy is again found to be an inappropriate metric. The impactor energies were not equivalent at the minimum compressive residual strengths for the three impactor masses used in the test program. The impactor energies corresponding to these minima were: 30 J for the 1523 g mass, 25 J for the 578 g mass, and 13 J for the 8.4 g mass.

Since damage tolerance, and therefore residual strength, is a function of the damage present, it was hypothesized that the same damage state exists for the minimum compressive residual strength condition for all three impactor masses. One measure of the damage characteristics used for correlation to compressive residual strength was determined from the X-ray photographs of each impact coupon. The information provided by an X-ray photograph is a summary of damage integrated through-the-thickness. These measurements represent the extent of this integrated damage as seen in the plane of the photograph. As seen previously in Figure 5, these measurements include the major and minor axes of the outer fringe of delamination as well as the diameter of the "core" area. The measurement of the major axis of damage did not include the spalling of fibers off the back surface to the coupon edge as this was a surface phenomenon.

Comparison of the compressive residual strength versus major axis of damage, presented in Figure 10, shows the curve for the 8.4 g impactor mass approaching the minimum compressive residual strength at a much smaller major axis of damage size (approximately 40 mm) than the curves for the 1523 and 578 g impactor masses (approximately 70 mm). There was a significant amount of scatter among the three impactor masses. Comparison of the compressive residual strength versus minor axis of damage, presented in Figure 11, resulted in less scatter than the major axis data comparison. Though the largest scatter band of data still represented a total difference of 33%, there was no obvious separation of data between the three impactor masses as there was in the case of the major axis. Comparison of the compressive residual strength versus core damage size, presented in Figure 12, also showed the curve for the 8.4 g impactor mass approaching the minimum compressive residual strength at a smaller core damage size (13 mm) than the curves for the 1523 and 578 g impactor masses (23 and 19 mm respectively). There was again, a significant amount of scatter among the three impactor masses. From these three comparisons, it would be inadvisable to predict compressive residual strength as a function of planar damage measurements such as the major axis, minor axis, or core damage size as there is insufficient detail in these damage measurements.

This can be further seen in Figure 13 where the X-ray characterization of the damage state at the minimum compressive residual strength condition is shown for the three impactor masses. These three cases appear to have slightly different damage states as the core damage size ranges from 17 to 23 mm, the minor axis of damage ranges from

21 to 27 mm, and the major axis of damage ranges from 69 to 80 mm. The integrated damage thus does not provide sufficient detail either in the X-ray photographs shown here, or in a typical ultrasonic scan. Three-dimensional information about the damage is therefore necessary.

The three-dimensional damage state definitions at the minimum compressive residual strengths for the three impactor masses used in this work were best provided by the deply destructive damage evaluation method. The cross-section schematics also provided good definition of the three-dimensional damage state. However, this destructive evaluation method was much more time consuming and labor intensive [27]. The comparison of the three-dimensional damage state definitions by deply are similar for specimens impacted by all three masses as shown in Figures 14–16. All three summaries exhibit similar damage type, size, shape, orientation, and location. Core damage remains fairly constant through the thickness due to impact at velocities in the penetration range. Delaminations exist between every interface with the exception of interface 6 (between the two 0° plies). Delamination shape is roughly elliptical with orientation in the direction of the next ply further away from the impact surface. Delamination size increases as ply distance from the impact surface increases. And, there is consistent evidence of extensive delamination between plies 1 and 2 including indications of the back surface spalling.

The similar deply summaries of Figures 14–16 would appear to verify the hypothesis that similar minimum compressive residual strengths are due to the existence of similar three-dimensional damage states in these specimens. These summaries, however, still do not identify the controlling or key damage mechanisms.

A postmortem examination of the specimens that failed at the minimum compressive residual strengths for the three impactor mass cases was conducted to determine if the failure modes were the same. These specimens, after failure, are shown in Figure 17. The postmortem examination of these minimum compressive residual strength specimens showed sublaminate buckling of ply 1 and fiber failure in the remaining plies. (Also evident was the extensive core damage and back side spalling of ply 1 due to impactor penetration.) Although it was not possible from the postmortem examination to determine which damage mode or combination of damage modes were controlling the compressive residual strength, it was clear that the failure modes in these three cases were similar if not the same. The postmortem examination of the open hole specimens on the other hand, showed the fracture in these cases to be consistently due to in-plane mechanisms as catastrophic failure occurred completely through each facesheet with no indication of delamination as shown in Figure 18.

Comments on Damage Evaluation Methods

It is apparent that there is a key need to determine the damage state in a composite structure subjected to impact in order to determine residual performance capabilities such as strength. Several two- and three-dimensional methods were used in this work. Two-dimensional methods included X-ray enhanced via dye penetrant and pulse-echo ultrasound. Three-dimensional methods included time-of-flight pulse-echo ultrasound, deply enhanced via dye penetrant, and cross-sectioning followed by microscopy.

The two-dimensional techniques provide a characterization of the damage which is integrated through-the-thickness. These techniques were inadequate in two respects.

One, the results were somewhat inconsistent as well as difficult to evaluate, as they require interpretation of the meaning of shades of gray or color. Two, this through-the-thickness integrated picture does not provide sufficient information to characterize the damage. The location of particular types of damage, such as delamination, is generally important in determining the residual performance of the laminate. This may become more important as the thickness of the laminate increases. Plots of residual strength versus planar damage size are therefore insufficient in representing the phenomena. Such plots require an assumption as to the configuration, types, and location of the damage.

It is therefore necessary to resort to techniques which provide accurate three-dimensional characterization of the damage state. Two destructive methods, cross-sectioning and deply, were used successfully in this work. The deply technique is preferred as it provides virtually complete damage information and is less labor-intensive than the cross-sectioning technique. However, neither of these techniques is an option to characterize damage in a production part or in a specimen which will be subsequently tested.

Time-of-flight ultrasonic pulse-echo scanning was performed on specimens to provide three-dimensional damage characterization via a nondestructive technique. A summary of the results of such an inspection is shown in Figure 19 for a specimen impacted at 70 m/s with an 8.4 g mass. This is the same specimen which was deplied and the damage summarized in Figure 16. The two damage summaries can therefore be directly compared. In this case, the core damage and delamination sizes seen via the time-of-flight technique are consistently larger than those seen via the deply technique. However, in general the damage sizes found via the time-of-flight technique were inconsistent with respect to the damage determined by the deply or cross-sectioning techniques.

The time-of-flight technique is limited by two other issues. One, damage "below" other damage cannot be detected. This can be somewhat mitigated by scanning from both sides of the specimen, but a complete picture may not always be possible. Two, these three-dimensional results also require interpretation of shades of gray or color as in the two-dimensional case. This latter difficulty may be overcome through continued experimentation and accumulated experience.

There is, therefore, great need to further develop nondestructive techniques to evaluate damage on a three-dimensional level in order to provide, with confidence, an accurate assessment of the damage state in the composite structure. Only this will allow proper assessment of the residual performance capability of the structure.

SUMMARY

The damage tolerance of composite laminates after impact was examined via experimentation on AS4/3501-6 graphite/epoxy laminates in a $[\pm45/0]_{2S}$ configuration. Three different impactor masses were used. The results clearly show that a minimum compressive residual strength exists which is well below the strength of a similar specimen with a 12.7 mm diameter open hole, the same diameter as the impactors. At higher impactor velocities, the compressive residual strength asymptotes to this open hole strength value. This minimum compressive residual strength is independent of the

impactor mass used and is directly related to the three-dimensional damage state in the specimen. Nondestructive and destructive examination showed that the damage state that caused the minimum compressive residual strength was the same for all three cases of impactor mass. This damage consists of a core region, where matrix and fiber damage occurs, and a delamination at every interface except between the two 0° plies. The delamination shapes are roughly elliptical and are oriented in the direction of the next ply further away from the impact surface.

This work clearly shows the need for proper metrics to measure impact damage in order to relate damage to the residual performance capability. It is clear that a full three-dimensional characterization of the damage is necessary rather than an integrated two-dimensional measure. Correlations to various two-dimensional impact metrics, such as the major axis of damage, were unsuccessful. Therefore, methods developed to predict residual performance should be based on the actual three-dimensional damage state. Furthermore, the inadequacies of the nondestructive techniques used demonstrate the need for further development of nondestructive techniques to properly characterize damage in laminated composite structures.

ACKNOWLEDGMENTS

REFERENCES

1. Cairns, D. S., and P. A. Lagace, "A Consistent Engineering Methodology for the Treatment of Impact in Composite Materials," Proceedings of the American Society for Composites, Fifth Technical Conference, East Lansing, Michigan, June, 1990, pp. 589–599.

2. Wilkins, D. J., "The Engineering Significance of Defects in Composite Structures," Characterization, Analysis and Significance of Defects in Composite Materials, AGARD-CP-355, 1983, pp. 20-1 through 20-11.

3. Potter, R. T., "The Significance of Defects and Damage in Composite Structures," Characterization, Analysis and Significance of Defects in Composite Materials, AGARD-CP-355, 1983, pp. 17-1 through 17-10.

4. Garg, A. C., "Delamination—A Damage Mode in Composite Structures," Engineering Fracture Mechanics, Vol. 29, No. 5, 1988, pp. 557–584.

5. Sollars, T. A., "Shuttle/Centaur G-Prime Composite Adapters Damage Tolerance/Repair Test Program," Proceedings of the 28th AIAA/ASME/ASCE/AHS Structures, Structural Dynamics and Materials Conference, Monterey, California, April, 1987, pp. 362–375.

6. Rhodes, M. D., J. G. Williams, and J. H. Starnes Jr., "Effect of Low-Velocity Impact Damage on the Compressive Strength of Graphite-Epoxy Hat-Stiffened Panels," NASA TN D-8411, April, 1977.

7. Baker, A. A., R. Jones, and R. J. Callinan, "Damage Tolerance of Graphite/Epoxy Composites," Composite Structures, Vol. 4, No. 1, 1985, pp. 15-44.

8. Whitehead, R. S., "Certification of Primary Composite Aircraft Structures," New Materials and Fatigue Resistant Aircraft Design, Proceedings of the 14th ICAF Symposium, Ottawa, Canada, June, 1987, pp. 585-617.

9. Byers, B. A., "Behavior of Damaged Graphite/Epoxy Laminates Under Compression Loading," NASA-CR-159293, August, 1980.

10. O'Brien, T. K., "Toward a Damage Tolerance Philosophy for Composite Materials and Structures," Composite Materials: Testing and Design, Vol. 9, ASTM STP 1059, 1990, pp. 7-33.

11. Challenger, K. D., "The Damage Tolerance of Carbon Fiber Reinforced Composites—A Workshop Summary," Composite Structures, Vol. 6, No. 4, 1986, pp. 295-318.

12. Flanagan, G., "Two-Dimensional Delamination Growth in Composite Laminates Under Compression Loading," Composite Materials: Testing and Design, ASTM STP 972, 1988, pp. 180-190.

13. Pavier, M. J., and W. T. Chester, "Compression Failure of Carbon Fibre-Reinforced Coupons Containing Central Delaminations," Composites, Vol. 21, No. 1, January, 1990, pp. 23-31.

14. Demuts, E., R. S. Whitehead, and R. B. Deo, "Assessment of Damage Tolerance in Composites," Composite Structures, Vol. 4, No. 1, 1985, pp. 45-58.

15. Garrett, R. A., "Effect of Defects on Aircraft Composite Structures," McAir No. 83-010, Presented at AGARD Structures and Material Panel, London, England, April, 1983.

16. Starnes, J. H., Jr., M. D. Rhodes, and J. G. Williams, "Effect of Impact Damage and Holes on the Compressive Strength of a Graphite/Epoxy Laminate," Nondestructive Evaluation and Flaw Criticality for Composite Materials, ASTM STP 696, 1979, pp. 145-171.

17. Ilcewicz, L. B., E. F. Dost, and R. L. Coggeshall, "A Model for Compression After Impact Strength Evaluation," Advanced Materials: The Big Payoff, 21st International SAMPE Technical Conference, Atlantic City, New Jersey, September, 1989, pp. 130-147.

18. Levin, K., "Effect of Low-Velocity Impact on Compressive Strength of Quasi-Isotropic Laminate," Proceedings of the American Society of Composites, First Technical Conference, Dayton, Ohio, October, 1986, pp. 313-326.

19. Guynn, E. G., and T. K. O'Brien, "The Influence of Lay-Up and Thickness on Composite Impact Damage and Compression Strength," Proceedings of the 26th AIAA/ASME/ASCE/AHS Structures, Structural Dynamics and Materials Conference, Orlando, Florida, April, 1985, pp. 187–196.

20. Williams, J. G., "Effect of Impact Damage and Open Holes on the Compression Strength of Tough Resin/High Strain Fiber Laminates," Tough Composite Materials, NASA-CP-2334, May, 1983, pp. 61–79.

21. Clark, G., and T. J. van Blaricum, "Carbon Fibre Composite Coupons - Static and Fatigue Behavior After Impact Damage," Structures Report 422, DSTO Aeronautical Research Laboratories, Melbourne, Australia, 1986.

22. Martin, R. C., and C. Poelman, "Compressive Residual Strength of Composite Laminates After Impact," 16.622 Final Report, Department of Aeronautics and Astronautics, Massachusetts Institute of Technology, December, 1989.

23. Dost, E. F., L. B. Ilcewicz, and J. H. Gosse, "Sublaminate Stability Based Modeling of Impact-Damaged Composite Laminates," Proceedings of the American Society for Composites, Third Technical Conference, Seattle, Washington, September, 1988, pp. 354–363.

24. Cairns, D. S., "Impact and Post-Impact Response of Graphite/Epoxy and Kevlar/Epoxy Structures," TELAC Report No. 87-15, Massachusetts Institute of Technology, August, 1987.

25. Freeman, S. M., "Characterization of Lamina and Interlaminar Damage in Graphite/Epoxy Composites by the Deply Technique," Composite Materials: Testing and Design, ASTM STP 787, 1982, pp. 50–62.

26. Williams, J. G., T. K. O'Brien, and A.J. Chapman III, "Comparison of Toughened Composite Laminates Using NASA Standard Damage Tolerance Tests," ACEE Composite Structures Technology, NASA-CP-2321, Seattle, Washington, August, 1984, pp. 51–73.

27. Guy, T. A., "Compressive Residual Strength of Graphite/Epoxy Laminates After Impact," TELAC Report No. 91-9, Massachusetts Institute of Technology, June, 1991.

28. Lagace, P. A., and A. J. Vizzini, "The Sandwich Column as a Compressive Characterization Specimen for Thin Laminates," Composite Materials: Testing and Design, ASTM STP 972, Philadelphia, Pennsylvania, 1988, pp. 143–160.

Table 1. Impact Test Matrix

Mass (g)	Velocity (m/s)	Test Type[a]		
		CRS	Section	Deply
1523	4.3	1[b]	—	—
	4.6	1	—	—
	4.8	3	—	—
	5.2	4	—	—
	5.5	3	1	—
	5.7	3	3	1
	6.0	4	2	—
	6.3	4	3	1
	6.7	3	2	—
	7.1	2	—	—
	7.5	2	1	—
	8.6	1	—	—
578	7.5	2	—	—
	8.0	2	3	—
	8.6	3	3	1
	9.2	6	3	1
	10.0	7	2	—
	10.9	3	1	—
	12.0	1	1	—
8.4	55	2	3	1
	56	1	1	—
	57	2	2	1
	58	1	3	1
	70	3	—	1

[a] CRS – compressive residual strength test after impact
Section – destructive damage evaluation by cross-sectioning
Deply – destructive damage evaluation by deply technique

[b] Indicates number of coupons tested

Table 2. Test Matrix and Results for Undamaged Specimens and Specimens with Open Holes

Diameter (mm)	Number of Specimens	Mean Compressive Strength (MPa)	Coefficient of Variation (%)
0.0	2	645	2.3
12.7	3	332	3.1
19.1	3	285	4.2
25.4	3	268	10.1
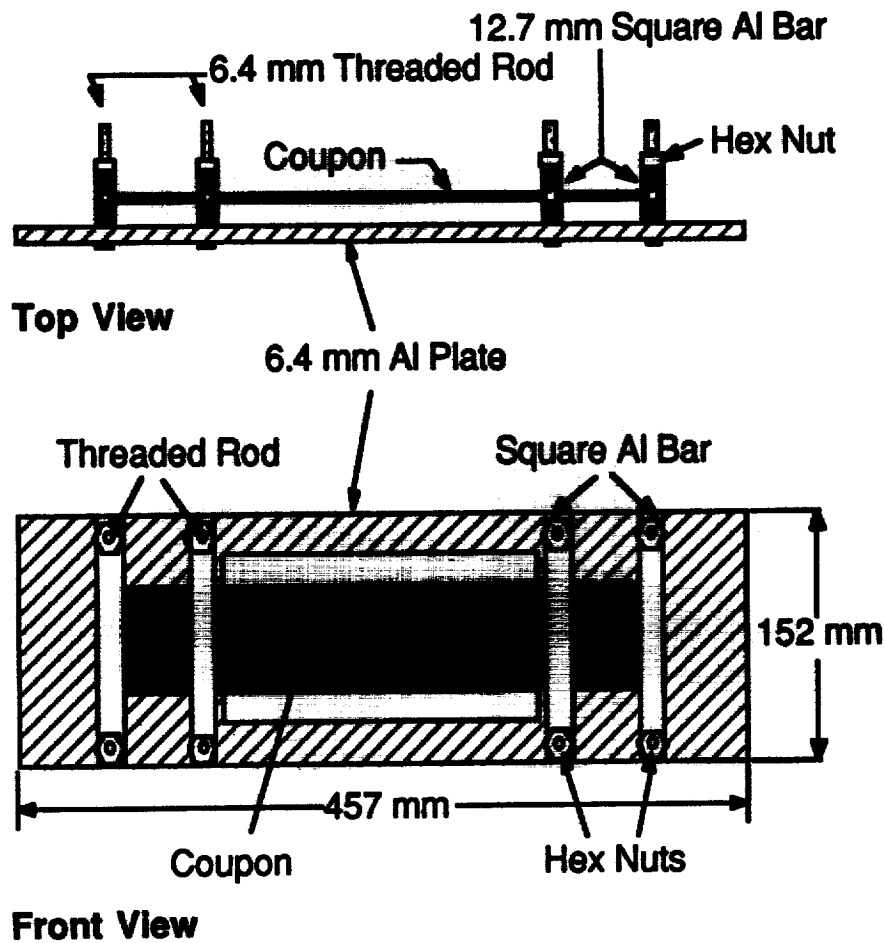
Figure 1. Illustration of Coupon Holding Jig for Impact Tests.
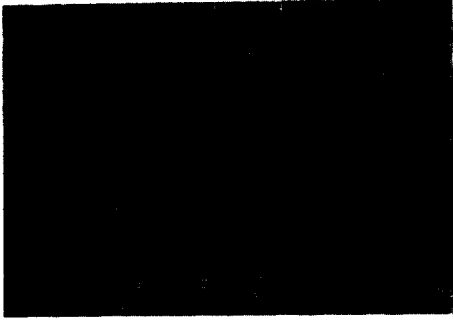
(X-ray is to scale)

Figure 4. Typical X-ray Photograph of Impact Damage.
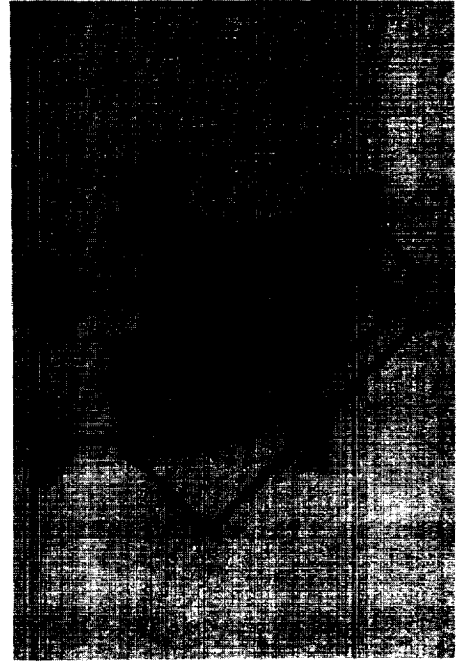
Figure 5. Schematic of Typical Damage Regions Illustrated by X-ray.

Figure 2. Illustration of Free Rolling Energy Device (FRED)
Impact Test Apparatus and Setup.
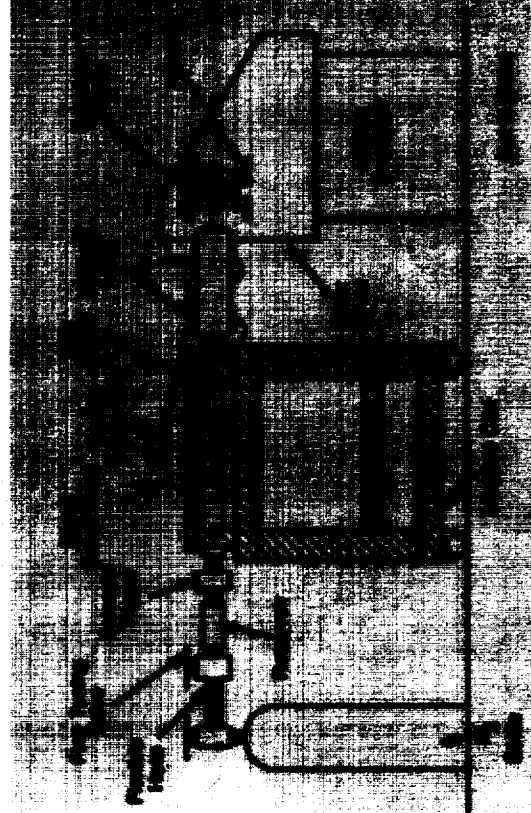
Figure 3. Illustration of Air Gun Impact Test Apparatus and Setup.

267

(Scale in picture is in mm)

Figure 6. Typical Photograph of Coupon Cross-Section through the Center of Impact.
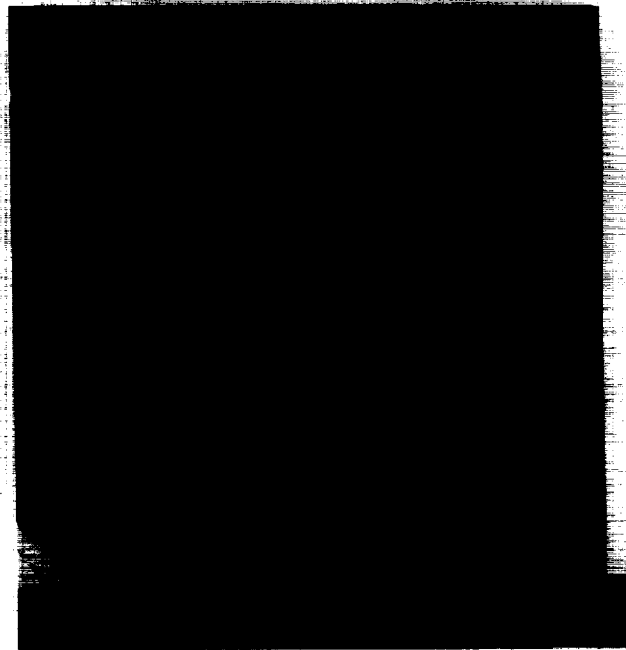
[45//-45/0/45/-45/0/0/-45/45/0/-45/45]—Impact Surface

(Scale in picture is in mm)

Figure 7. Typical Photograph of Ply Surface After Deply.
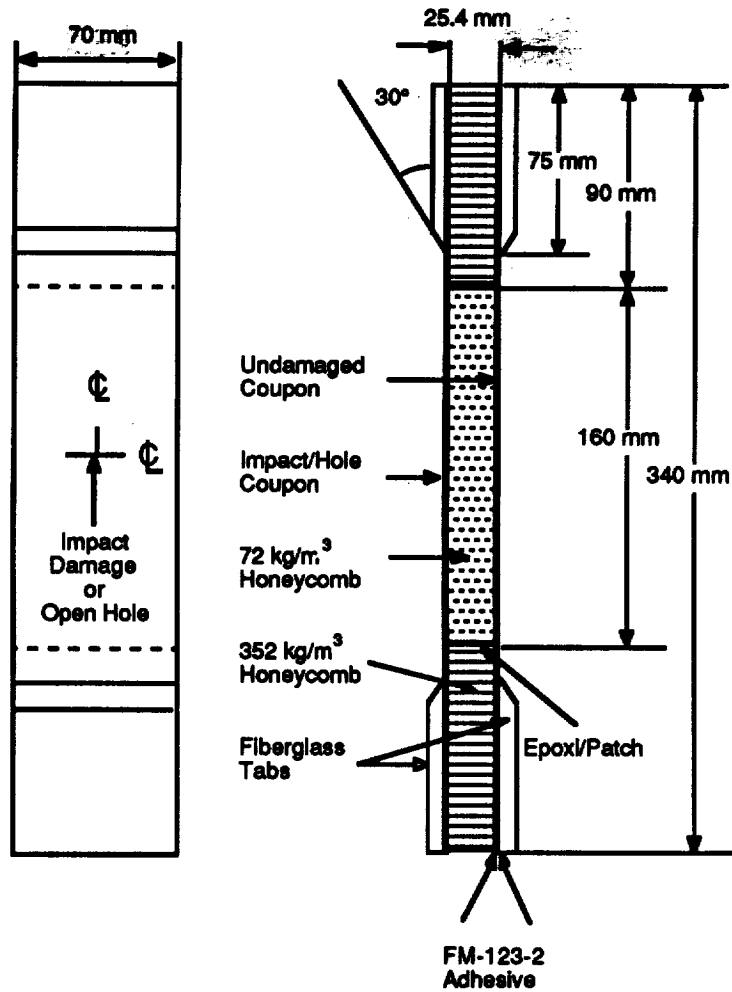
Figure 8. Compressive Residual Strength Test Specimen Geometry.
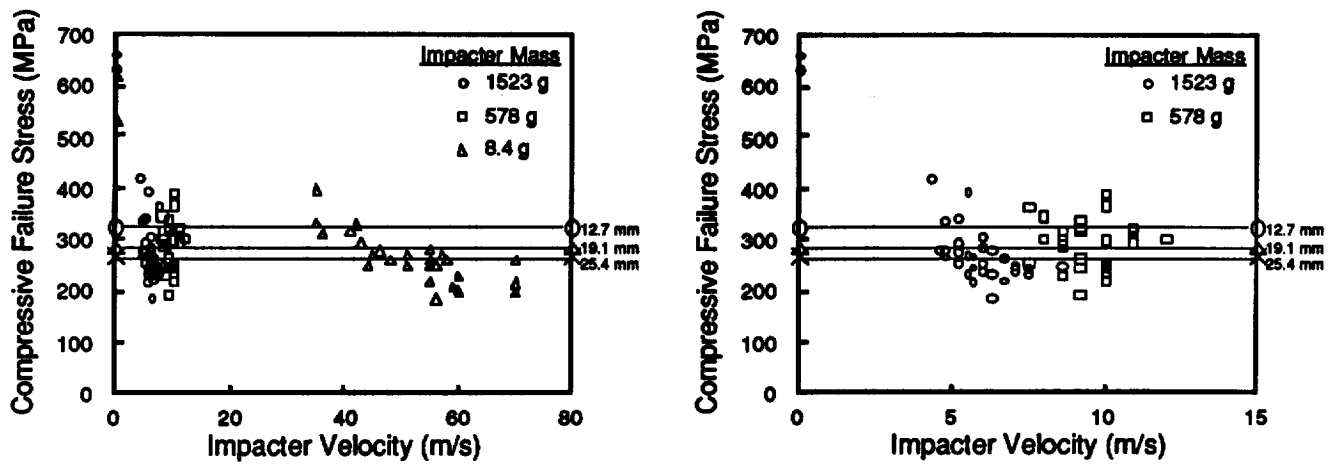
Figure 9. Compressive Residual Strength versus Impacter Velocity Data-
(*left*) three impactor masses, (*right*) 1523 g, 578 g impactor masses.

269
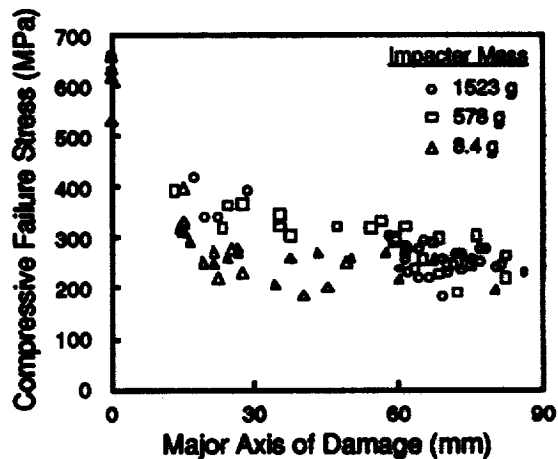
Figure 10. Compressive Residual Strength versus Major Axis of Damage Data.
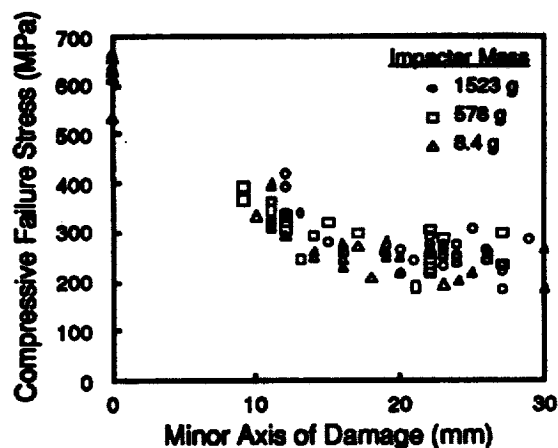
Figure 11. Compressive Residual Strength versus Minor Axis of Damage Data.
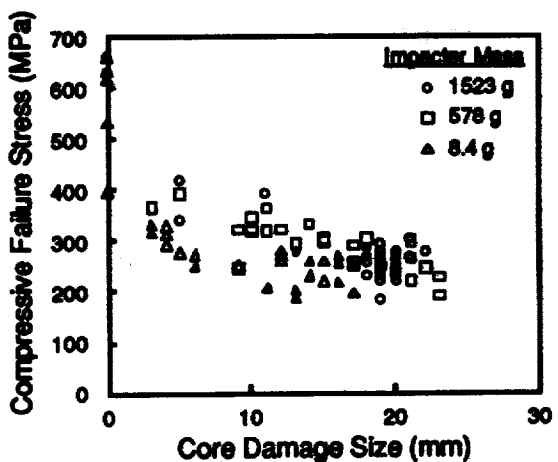
Figure 12. Compressive Residual Strength versus Core Damage Size Data.

Mass = 8.4 g   Mass = 578 g

Mass = 1523 g

(X-rays are to scale)

Figure 13. X-ray Photographs of Minimum Compressive Residual Strength Specimens
for Three Impacter Masses (*top left*) 8.4 g, (*top right*) 578 g, and (*bottom*) 1523 g.
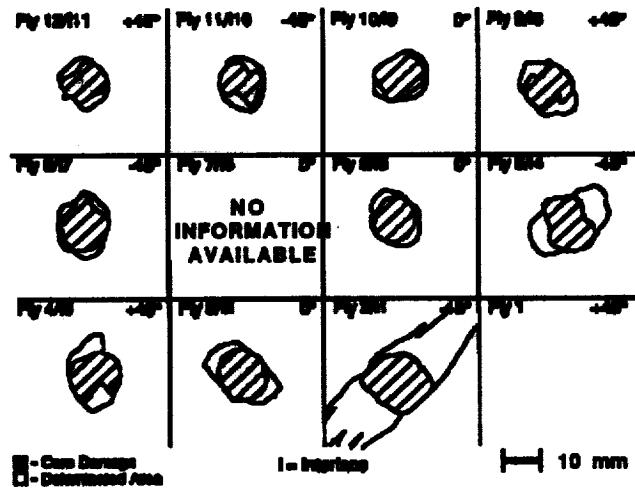
Figure 14. Summary of Damage Observed in Specimen M8-2 by Deply (Impacter Mass = 1523 g, Velocity = 6.3 m/s).
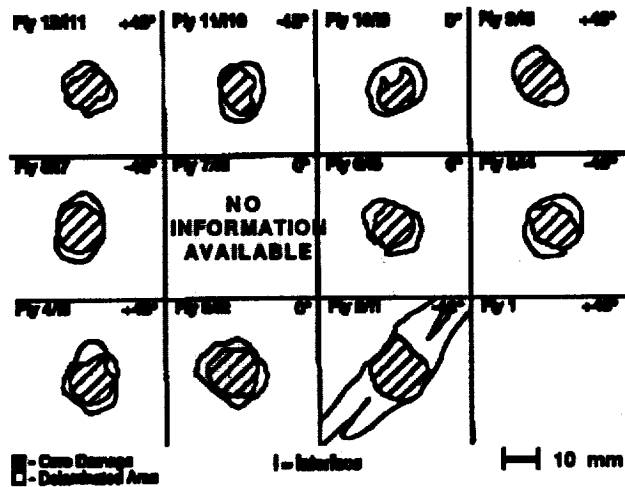
Figure 15. Summary of Damage Observed in Specimen M10-4 by Deply (Impacter Mass = 578 g, Velocity = 8.6 m/s).
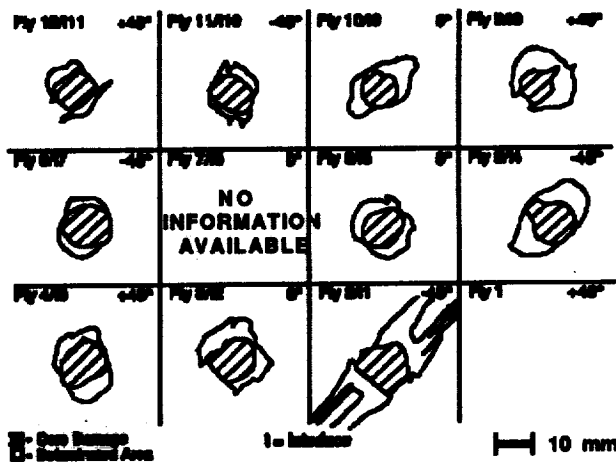

Figure 16. Summary of Damage Observed in Specimen M23-4 by Deply (Impacter Mass = 8.4 g, Velocity = 70 m/s).

272
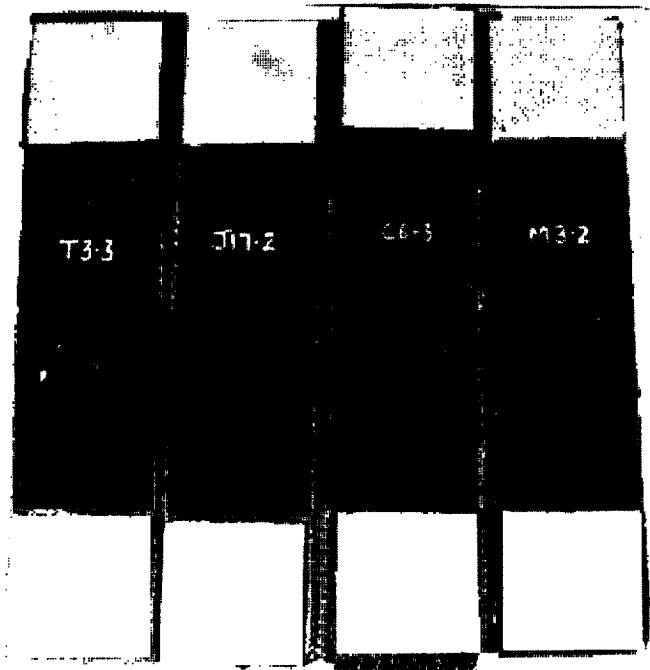
(Mass of 1523 g at 6.3 m/s)
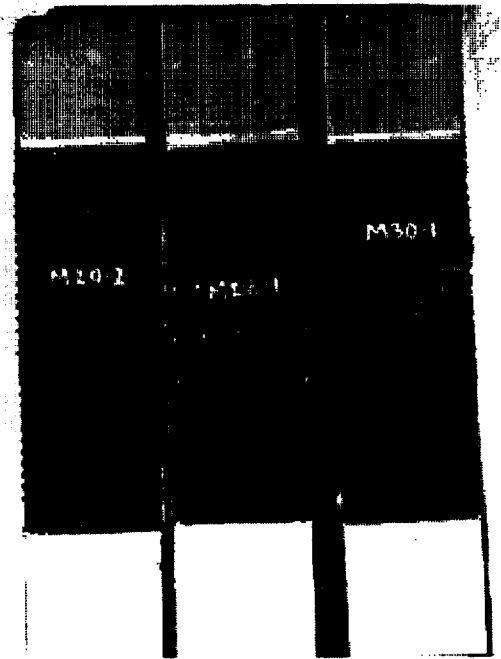
(Mass of 8.4 g at 70 m/s)

(Mass of 578 g at 9.2 m/s)

(Specimens - 70 x 340 mm)

Figure 17. Photograph of Impact-Damaged Specimens After Fracture
Masses of (*top left*) 1523 g, (*bottom*) 578 g, and (top *right*) 8.4 g.
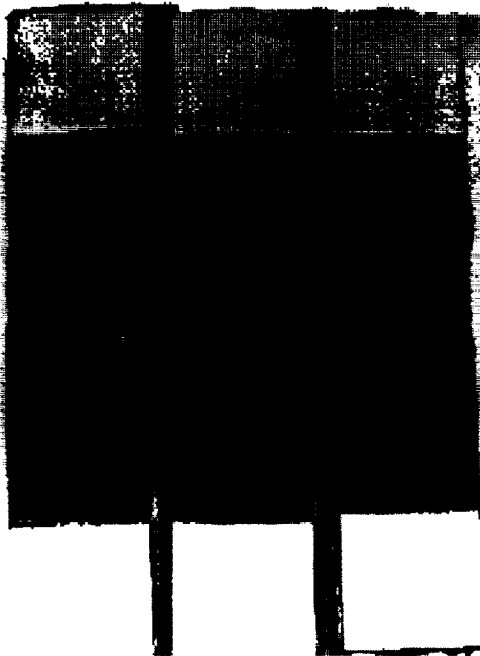
(Specimens - 70 x 340 mm)

Figure 18. Photograph of 12.7 mm Open Hole Specimens After Fracture.
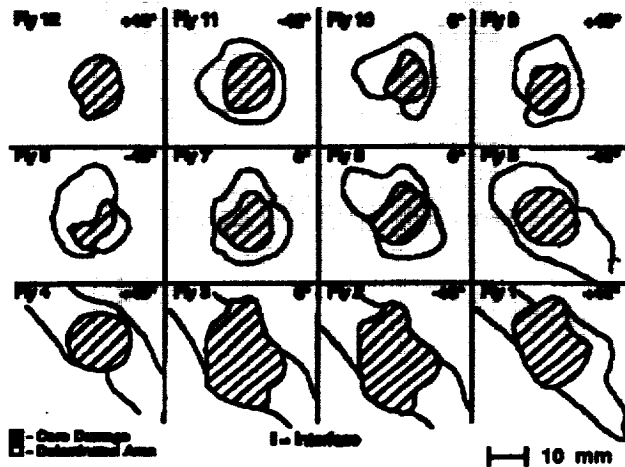
Figure 19. Summary of Damage Observed in Specimen M23-4 by Time-of-Flight
Ultrasonic C-Scan (Impacter Mass = 8.4 g, Velocity = 70 m/s).

SESSION III

DESIGN APPLICATIONS (A)

THIS PAGE INTENTIONALLY BLANK